

A New 3D Active Camera System for Robust Face Recognition by Correcting Pose Variation

°Young-Ouk Kim, °Sung-Ho Jang , °Chang-Woo Park, °Ha-Gyeong Sung, °Ohyun Kwon and °Joonki Paik

° Precision Machinery Center, Korea Electronics Technology Institute, 401-402 B/D
192, Yakdae-Dong, WonMi-Gu, Puchon-Si, KyungGi-Do 420-140, Korea
(Tel : +82-32-621-2847; E-mail : kimyo@keti.re.kr)

°Image Processing and Intelligent Systems Laboratory, Department of Image Engineering,
Graduate School of Advanced Imaging Science, Multimedia, and Film,
Chung-Ang University, 221 Huksuk-Dong, Tongjak-ku, Seoul 156-756, Korea.
(Tel : +82-2-820-5300; E-mail : paikj@cau.ac.kr)

Abstract : Recently, we have remarkable developments in intelligent robot systems. The remarkable features of intelligent robot are that it can track user, does face recognition and vital for many surveillance based systems. Advantage of face recognition when compared with other biometrics recognition is that coerciveness and contact that usually exist when we acquire characteristics do not exist in face recognition. However, the accuracy of face recognition is lower than other biometric recognition due to decrease in dimension from of image acquisition step and various changes associated with face pose and background. Factors that deteriorate performance of face recognition are many such as distance from camera to face, lighting change, pose change, and change of facial expression. In this paper, we implement a new 3D active camera system to prevent various pose variation that influence face recognition performance and propose face recognition algorithm for intelligent surveillance system and mobile robot system.

Keywords: Active cameras, face segmentation, pose estimation, robust Hausdorff distance.

1. INTRODUCTION

This paper discusses the experimental result of a new 3D active camera system for face recognition and precise face segmentation method. The area of face recognition has become more important than ever before because of the increasing needs for security. Eigenface (PCA) [1] and Local Feature Analysis (LFA) [2] are popular algorithms used in face recognition technology. Other algorithms such as Linear Discriminant Analysis (LDA) [3], Independent Component Analysis (ICA) [4], Elastic Graph Matching (EGM) [5], Neural Networks (NN) [6], Support Vector Machines (SVM) [7] and Hidden Markov Models (HMM) [8] were also actively investigated for face recognition. Although some leading (according to the FERET Evaluation Report [9]) commercial software packages such as the one by Identix (formerly Visionics) and Viisage are widely used in real applications such as in super bowl games and airports, critics have believed that the accuracy is still questionable.

The performance of any face recognition software depends on how one controls the area in which faces are captured in order to minimize illumination effects, pose and other facial variations [10]. A performance enhancement technique has been proposed using the post-processing method in [11]. Among various factors that directly affect the accuracy of a face recognition algorithm, the pose of the face is the most important in terms of quality and reliability of outcome [12].

A face feature extraction method can be either appearance based or feature point based. The appearance based method that calculates the characteristic amount of features and the feature based method that uses the geometrical relationship between features and comparison with texture information of eyes, nose and mouse. Statistical learning methods such as PCA/LDA have been commonly used in face recognition of image data. In case of face data bases, it consists of front side view that leads good performance.

However, these methods based on whole face image information has disadvantages such as difficulties for acquiring whole facial face data caused by pose, illumination

and expression changes. Exact pose estimation is essential to compensate the face pose variation which influences the recognition ability [12]. If the pose deviation from the frontal view is greater than $\pm 25^\circ$, the less accuracy achieved and the more manual aligning required.

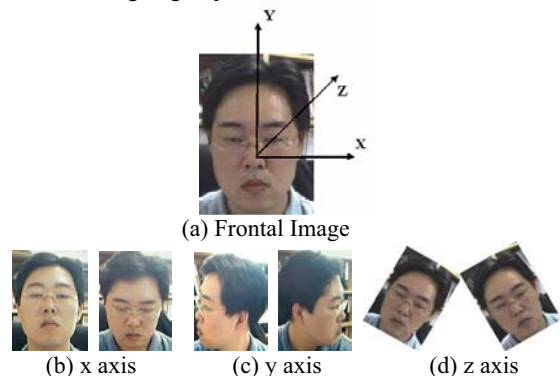


Fig. 1 Pose variation of face

In case of Fig. 1 (d, rotated z axis) we can simply transform frontal view image using affine transform and eye detection method. In the Fig 1.(b) and (c) face is rotated by x axis and y-axis, and transformation is introduced using 3 dimensional modeling in these cases. The various pose estimation method and the comparison of methods was introduced in [13]. In this paper, pose estimation is approached to coarse a probabilistic model approach and a neural network approach.

The probabilistic model approach is more robust for face localization accuracy but does not perform well on very low-resolution face images. Most of these algorithms meet the complexity problem but are computationally very slow and not realizable in real time.

This paper describes a new active camera system for face recognition by correcting pose variation which uses statistical method preserving the image resolution.

In section 2, we introduce a new 3D active camera system with segmentation a body and face candidate area. A small pan/tilt camera is implemented for real-time face tracking

using template matching and color segmentation. We can segment the face area accurately from complex background.

We describe a feature extraction method that is affected less in color and brightness change of face in the natural scene in section 3. It is very important when the face recognition runs under the appearance based approach. Also, we implement fixed size of face data bases to use face recognition process.

In section 4, we present the pose estimation process using a simple fuzzy logic and positioning method of active camera to get almost frontal face image.

Finally, section 5 presents the simulation result compared to general PCA and HMM process having various rotated faces from x and y axis.

The Figure 2 shows the overall process of this research.

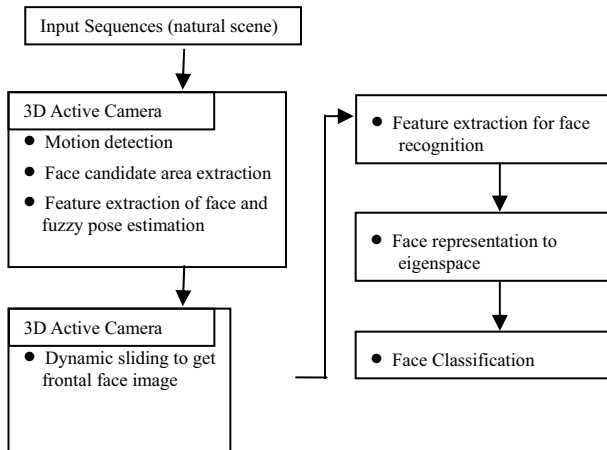


Fig. 2 Pose estimation and recognition flowchart

2. THE 3D ACTIVE CAMERA SYSTEM

2.1 System overview 3D Active camera.

To estimate the pose form rotated form face images, geometrical transform method using statistical data is used normally.

However, in this method occurrence of the facial information loss leads occasionally to lower performance such as PCA and LDA method using image base approach. Some papers introduced to prevent this problem using multiple cameras. Nonetheless, in this paper using a 3D active camera has ability to rotate pan(y axis)/tilt(x axis) direction and to slide into x direction for pose compensation by hardware movement.

The degree of pan is from -90° to 90° and tilt is from -30° to 30° . The Table 1 and Figure 3 show result of pose test [12].

Table 1: Summary of pose test

Pose(R, L)	1st Match (%)	1 st 10 Match (%)	Manual Aligning Required (%)
90°L	N/A	N/A	100.0
60°L	34.5	71.0	13.5
40°L	65.0	91.0	4.5
25°L	95.0	99.5	2.5
15°L	97.5	100.0	0.5
0	100.0	100.0	0.0
15°R	99.0	99.5	0.0
25°R	90.5	99.5	2.0
40°R	61.5	87.5	4.5
60°R	27.5	65.0	11.0
90°R	N/A	N/A	100.0

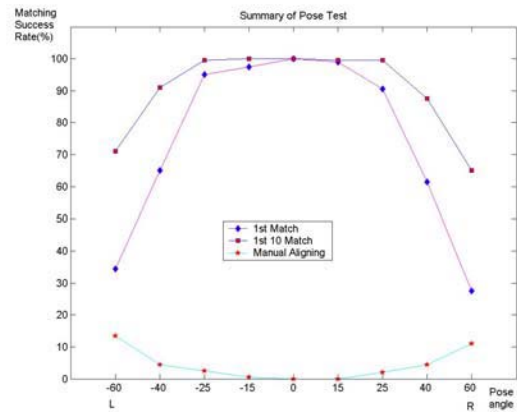


Fig. 3 Summary of pose test

In the Figure 3, if the pose variation is greater than $\pm 25^\circ$ a matching rate becomes low. But our 3D active camera can align x and y axis direction up to $\pm 45^\circ$. Figure 4 present the concept of 3D active camera.

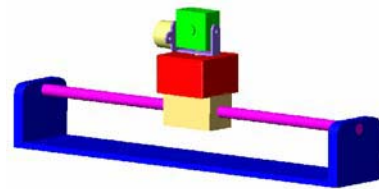


Fig. 4 3D active camera

The 3D active camera has 1200mm slide length to compensate $\pm 45^\circ$ rotated faces when the distance between face and camera is below 60cm. Our 3D active camera has two constraints which are the distance with camera and face must be 0.6m below and the y axis rotation angle must be $\pm 45^\circ$ below. However, we can acquire front side image without these limitation in case of mobile robot system.

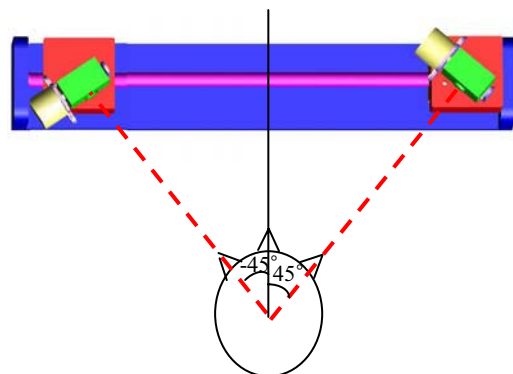


Fig. 5 Constraint of the 3D active camera

Figure 5 present the basic idea for pose localization and its constraint. The face tracking process is continued while image sequences are acquired and pose estimation process is achieved once every two seconds by fuzzy inference it will be describe in detail chap 4. Then we can control sliding axis according to the pose variation and x, y axis to acquire frontal face image.

To localize face pose, robust face tracking is applied using pan/tilt active camera mounted in figure 5. It is composed

motion detection and face segmentation.

2.2 Motion detection and face segmentation.

Robust face tracking is also challenging fields in computer vision as well as pose estimation. We simply illustrate the skin and hair color reference map and limit our attention to the segmentation algorithm using convex hull [14].

The first work is classifying pixels of the frame p in video sequence into skin color and non-skin color. In order to do so, we use a skin color reference map in YCbCr color space like [15]. Let's define skin color range of Cb and Cr in YCbCr color space as R_{Cb} and R_{Cr} , respectively and we call the skin color range as skin color reference map. The $R_{Cb}=[77\ 127]$ and $R_{Cr}=[133\ 173]$ is defined by [15], which propose a set of regularization processes that are based on the spatial distribution and the corresponding luminance values of the detected skin color pixels and this approach overcomes the restriction of motion analysis and avoids the extensive computation of the ellipse-fitting method.

With this skin color reference map, the skin color segmentation can now begin. Let's call the set of pixel of frame extracted from the skin color reference map as the skin likeness region. Since we are utilizing only the color information, the segmentation requires only the chrominance component of the frame.

The skin color likeness is described as

$$S(x, y) = \begin{cases} 1, & \text{if } [Cb(x, y) \in R_{Cb}] \cap [Cr(x, y) \in R_{Cr}] \\ 0, & \text{otherwise} \end{cases} \quad (1)$$

For hair color segmentation, we make the hair color region in RGB color space. A race in this paper is limited as an oriental having black hair. Usually, the hair color has an insensitive property to luminance. Let's define hair color ranges of R, G and B in RGB color space as $R_R=[0\ 30]$, $R_G=[0\ 30]$ and $R_B=[0\ 30]$ in experience, respectively and we call the hair color range as hair color reference map. We extract the image points falling inside respective hair color reference map for hair color segmentation. Let's call the set of pixel of frame extracted from the hair color reference map as the hair likeness region. We can find the set of pixels of the hair likeness regions of a frame in video sequence from equation (2).

$$H(x, y) = \begin{cases} 1, & \text{if } [R(x, y) \in R_R] \cap [G(x, y) \in R_G] \cap [B(x, y) \in R_B] \\ 0, & \text{otherwise} \end{cases} \quad (2)$$

A convex polygon has the property that any line connecting any two points inside the polygon must itself lie entirely inside the polygon [15]. Then, we define set of points constructing the convex polygon as convex hull.

This paper proposed an effective face segmentation algorithm using the property of convex-hull. Usually, the skin and hair color regions with intersection of them have a very strong possibility that they may be the face and hair.

After assigning label to each color region, we make the set of the pixels in the convex-hull of hair color region as H_j and that of skin color region and intersection region as F_i , I_{ij} , respectively. ($i = 1 \sim n, j = 1 \sim m$)

$$I_{ij} = F_i \cap H_j$$

$$\text{Set the value of pixels in } F_i \quad \text{if } n[I_{ij}] > \tau \quad (3)$$

$$0 \quad \text{otherwise}$$

where, - $n[\cdot]$: the number of element in the set
- n and m denote the number of the set of the pixels in the convex-hull surrounding skin likeness regions and that of hair likeness regions

Figure.6 shows the face segmentation procedure via convex-hull in a frame. Using equation (3)



Fig. 6 Face segmentation algorithm

3 EIGENFACES FOR POSE ESTIMATION AND RECOGNITION

In this paper, we define two databases for face recognition. The first database is consisted by face angle to estimate face pose and to control the sliding axis in figure4. And the other is individual frontal view faces. To construct face databases we use multilayered edge map regardless of color special quality of input face candidate area in section 2.2.

3.1 Multilayered edge map for face database

There are elements such as eyes, eyebrows, nose, mouth, tip of nose, ears, and etc that display various face qualities in the feature. Eyes that are the most notable characteristic element among them are used as an important element in several studies.

Mouth can be prominent but because variability was the most serious among face components and difficulties in expressing by general quality based modeling error, there have been positions inference research in a measure that uses color quality detected by many red color in neighborhood lips and example applied to face recognition finding feature point of both side of the mouth under the high resolution situation

Eyes have darker quality than surrounding face area. In the case of usual eyes neighborhood, dark and small area is obtained by shape such as horizontal edge of close resemblance 'blob' form that has bigger length to horizontal direction. Even though mouth area has fairly darker area than neighborhood such as eyes area similarly, and the width of the area is more various than eyes area, the size does not differ greatly with that of eyes. In addition, horizontal edge of blob form in mouth appears more clearly in eyes neighborhood. Considering these gray intensity of a face element we are doing to infer the possible position of face element composing directional blob template [18].

The size of template would be decided by considering the size of face to be detected, but selected by the rate of longer width that is similar in eye size (Fig.7). Let's define $P_{cent}(x_c, y_c)$ as a center pixel in the pixel $P(x, y)$ which has image size of $W \times H$ and get luminosity deviations between I_{cent} (intensity of $P(x_c, y_c)$) and average luminosity \bar{I}_{Dir} of 8 directional pixel of face element template (size: $h_{FF} \times w_{FF}$) on the standard of P_{cent} calculating average luminosity like

eq(4)~(7).

$$\begin{aligned} \bar{I}_{Left} &= \left\{ \sum_{i=-w_{FF}/2+X_C}^{i=X_C} \sum_{y=Y_C}^{y=Y_C} P(x+i, y) / (w_{FF}/2) \right\} \\ \bar{I}_{Right} &= \left\{ \sum_{i=X_C}^{i=w_{FF}/2+X_C} \sum_{y=Y_C}^{y=Y_C} P(x+i, y) / (w_{FF}/2) \right\} \\ \bar{I}_{Top} &= \left\{ \sum_{x=X_C}^{x=X_C} \sum_{j=h_{FF}/2+Y_C}^{j=Y_C} P(x, y+j) / (h_{FF}/2) \right\} \\ \bar{I}_{Bottom} &= \left\{ \sum_{x=X_C}^{x=X_C} \sum_{j=-h_{FF}/2+Y_C}^{j=Y_C} P(x, y+j) / (h_{FF}/2) \right\} \end{aligned} \quad (4)$$

$$\begin{aligned} \bar{I}_{NW} &= \left\{ \sum_{i=X_C-h_{FF}/2}^{i=X_C} \sum_{j=-i}^{j=-i} P(x+i, y+j) / (h_{FF}/2) \right\} \\ \bar{I}_{NE} &= \left\{ \sum_{i=X_C}^{i=X_C+h_{FF}/2} \sum_{j=i}^{j=i} P(x+i, y+j) / (h_{FF}/2) \right\} \\ \bar{I}_{SW} &= \left\{ \sum_{i=X_C}^{i=X_C} \sum_{j=-i}^{j=-i} P(x+i, y+j) / (h_{FF}/2) \right\} \\ \bar{I}_{SE} &= \left\{ \sum_{i=X_C+h_{FF}/2}^{i=X_C} \sum_{j=-i}^{j=-i} P(x+i, y+j) / (h_{FF}/2) \right\} \end{aligned} \quad (5)$$

$$\begin{aligned} \Delta I_{width} &= (|I_{cent} - \bar{I}_{Left}| + |I_{cent} - \bar{I}_{Right}|) / 2 \\ \Delta I_{height} &= (|I_{cent} - \bar{I}_{Top}| + |I_{cent} - \bar{I}_{Bottom}|) / 2 \\ \Delta I_{Diag1} &= (|I_{cent} - \bar{I}_{NW}| + |I_{cent} - \bar{I}_{SE}|) / 2 \\ \Delta I_{Diag2} &= (|I_{cent} - \bar{I}_{NE}| + |I_{cent} - \bar{I}_{SW}|) / 2 \end{aligned} \quad (6)$$

$$\vec{d}_{Pr}, |\vec{d}_{Pr}| = \text{Max} \{ \Delta I_{width}, \Delta I_{height}, \Delta I_{Diag1}, \Delta I_{Diag2} \} \quad (7)$$

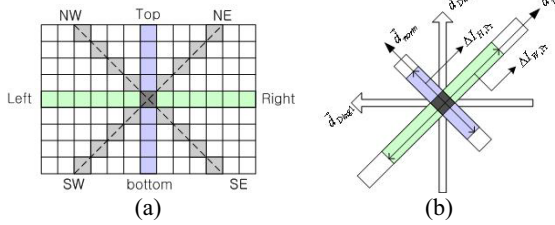
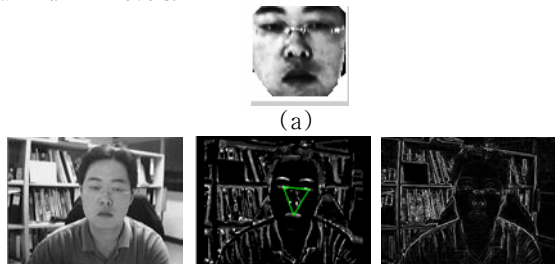


Fig. 7 (a) Directional intensity template (b) principal direction for creation of multilayered edge maps

The Fig.7(a) shows the example of these 8 direction template. Principal direction \vec{d}_{Pr} is defined as the highest part of the luminosity deviations and get deviation size $|\vec{d}_{Pr}|$. Using every pixel of main direction \vec{d}_{Pr} of deviation and deviation size $|\vec{d}_{Pr}|$ at that moment, directional template is applied again to whole image (fig.6(b) reference). Allocate edge strength of +1 level when the value $\Delta I_{w,Pr}$ calculated average image luminosity toward both \vec{d}_{Pr} directions is higher than the threshold which is the value allocated proper weighting factor on main directional deviation intensity. Next, in case of higher pixel than weighted pixel value that directs perpendicularity \vec{d}_{Norm} of the main direction it is one more time given the edge intensity +1(total +2). It is same for the both diagonal direction $\vec{d}_{Diag1,2}$ giving +1 edge intensity. Whole image through this process has multilayered edge map which has different strength of brightness according to the case which satisfies 4 step edge intensity condition and the gray edge is created in edge intensity position that is given to maximum +4 levels.



(b) (c) (d)
Fig. 8 (a) face database(60 x 60) (b) original image (CIF) (c) multilayered edge (d) sobel edge

3.2 Fuzzy inference for pose variation and SVD

In the section 3.1 we introduce a multilayered face edge map which aligned with nose position. The pose of x and y axis can be estimated using a simple PCA and Mamdani fuzzy inference.

We composed a face database having 15 degree from frontal view of face such as -45°, -30°, -15°, 0°, 15°, 30°, and 45°. In this research there need not be many databases for pose variation. We have only 5 images per each degree.



Fig. 8 Face database for pose estimation

In the process of PCA to estimate the pose we need covariance matrix C and its eigenvectors from training image sets. Let's $x_1, x_2, x_3, \dots, x_N$ are N training face vectors. Then, by definition, C can be estimated by [17]

$$C = E[XX^T] \cong \frac{1}{N} \sum_{k=1}^N X_k X_k^T. \quad (8)$$

The training dataset packed into matrix

$$X = [x_1, x_2, x_3, \dots, x_N] \quad (9)$$

then, the estimate of C can be written as

$$C \cong \frac{1}{N} XX^T \quad (10)$$

To find the eigenvectors of C , we just need to find the eigenvectors of XX^T . Even for images of moderate size, however, this is computational complex. The solution is to realize that [16], through a singular value decomposition (SVD) of X , the eigenvectors of XX^T can be found from eigenvectors of $X^T X$, which are much easier to obtain. Specifically, suppose the rank of X is r , $r \leq N$. According to linear algebra theory, X has an SVD

$$X = \sum_{k=1}^r \sqrt{\lambda_k} u_k v_k^T \quad (11)$$

Here, $\sqrt{\lambda_k}$, u_k and v_k are, respectively, singular values

and left and right singular vectors of X . $\sqrt{\lambda_k}$ are nonzero eigenvalues of XX^T and $X^T X$ and u_p (n by one vector) and v_p (N by one vector) are, respectively, the eigenvectors of XX^T and $X^T X$. This means (by multiplying both sides of (11) with v_k)

$$u_k = \frac{1}{\sqrt{\lambda_k}} X v_k \quad (12)$$

Hence, we can find eigenface u_k easily after finding v_k , which is relatively easy.

The pose variation of face is estimated using PCA and fuzzy inference engine. In this paper we present 7 inputs and 7 output fuzzy inference engine. The input of fuzzy are 7 distances from PCA and the outputs are angle of rotated face.

We can decide the amount of sliding distance in the figure 5.

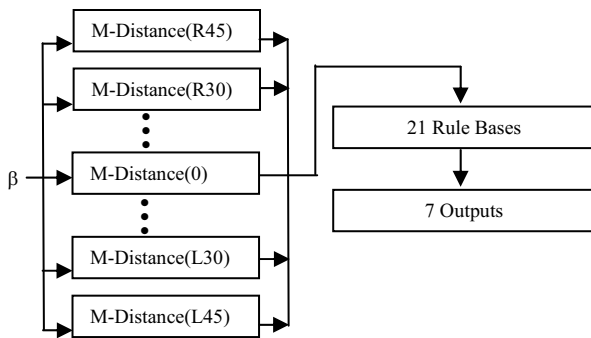


Fig. 9 Pose estimation using fuzzy logic

Where, β is coefficient of input vector which is inspected eigenspace.

The rule bases can be

$$\begin{array}{ll} \text{ZERO} & 1 \\ \text{If } D(R_\theta) \text{ is SMALL then } Output_\theta \text{ is } 0.5 & (13) \\ \text{LARGE} & 0 \end{array}$$

Where R_θ are $-45^\circ, -30^\circ, -15^\circ, 0^\circ, 15^\circ, 30^\circ, 45^\circ$.

The input membership function of fuzzy inference engine is presented figure 10.

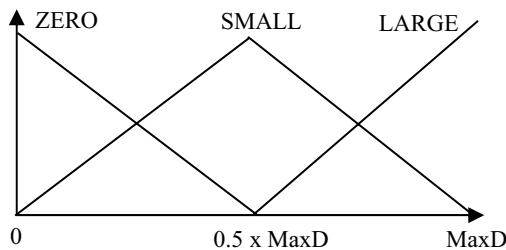


Fig. 10 Input membership function

The estimated face pose can be written

$$\begin{aligned} \text{Face Pose} = & -45^\circ(1/Output_{-45^\circ}) + -30^\circ(1/Output_{-30^\circ}) + \dots \\ & + 30^\circ(1/Output_{30^\circ}) + 45^\circ(1/Output_{45^\circ}) \quad (14) \end{aligned}$$

using singleton fuzzifier, product inference engine and average defuzzifier.

4. EXPERIMENTAL RESULTS

4.1 Result of pose estimation

The figure 11 preset our 3D active camera system.



Fig. 11 3D active camera system

In this first experiment for pose estimation, images were classified having such as $-45^\circ, -30^\circ, -15^\circ, 0^\circ, 15^\circ, 30^\circ$, and 45° degree. The use of 3D active camera enables movement in three dimensions. The table given below gives the result of the proposed pose estimation. The number of input samples for the data base is fixed at 156. It can be seen that very high correction percentage is achieved in almost all case. Though the trend follows that for increased angular variation the correction factor decreases slightly. Best results are seen for five degrees right to left variation.

Table 1 Results showing the performance of Pose variation.

Pose variation (R, L)	Input Samples	Correction (%)
40~50°R	156	92.3
25~35°R	156	95.6
10~20°R	156	98.1
5°R~5°L	156	99.2
10~20°L	156	98.3
25~35°L	156	93.4
40~50°L	156	92.5

4.2 Result of face recognition

In this section we present a comparative evaluation of our Pose variation algorithm with PCA and HMM method. The experiment was carried out on two sets of data sets as given in the Table 2. It can be seen the proposed method outperforms other methods for all pose angles. The PCA method on the second data set is better than that on the first data set. The Hidden Markov Model (HMM) is found to be equally efficient in low pose angular variations. But with increase in pose variation the proposed method proves to be most reliable and robust.

Table 2 Comparative evaluation of different pose variation methods.

Pose variation (R, L)	*Our method (%)	*PCA (%)	**HMM (%)	**PCA (%)
40~50°R	90.2	34.5	70.6	60.2
25~35°R	93.4	65.1	88.2	78.6
10~20°R	96.4	92.0	93.8	93.0
5°R~5°L	98.2	97.4	98.0	97.8
10~20°L	96.2	92.2	93.6	93.1
25~35°L	93.5	65.0	87.9	79.5
40~50°L	90.8	35.0	71.0	62.7

*: 70 persons, each with 10 front view images

** :70 persons, each with 70 different pose variation

5. CONCLUSIONS

This paper presented the development of 3D active camera system in order to overcome the performance degradation due to the face pose variation. The proposed face recognition system consists of motion detection, rough face region segmentation, novel accurate face detection via face features, and face recognition procedure using 3D active camera system.

Various face recognition performance evaluation using PCA and HMM based on the developed 3D active camera system was made. The experiments illustrated that the recognition performance using 3D active camera was higher than the existing methodologies in the case that the face pose variation exist severely.

REFERENCES

- [1] M. Turk and A. Pentland, "Eigenfaces for recognition," *Journal, Cognitive Neuroscience*, vol. 3, pp 72-86, 1991.
- [2] P. Penev and J. Attick, "Local Feature Analysis: a general statistical theory for object representation," *Network: Computation in Neural Systems*, vol. 7, no. 3, pp.447-500, 1996.
- [3] P. Belhumeur, J. Hespanha, and D. Kriegman, "Eigenfaces vs. fisherfaces: recognition using class specific linear projection," *IEEE Trans. PAMI*, vol. 19, no. 7, pp.711-720, 1997.
- [4] P. Comon, "Independent component analysis, a new concept?," *Signal Processing*, vol. 36, pp. 287-314, 1994.
- [5] L. Wiskott, J. Fellous, N. Krüger, and C. Malsburg, "Face Recognition by Elastic Bunch Graph Matching," *IEEE Trans. PAMI*, vol 19, pp. 775-779, 1997.
- [6] H. Rowley, S. Baluja, and T. Kanade, "Neural Network-Based Face Detection," *Proc. IEEE Conf. Computer Vision, Pattern Recognition*, pp. 203-208, 1996.
- [7] E. Osuna, R. Freund, and F. Girosi, "Training support vector machines: an application to face detection," *Proc. IEEE Conf. Computer Vision, Pattern Recognition*, pp. 130-136, 1997.
- [8] F. Samaria and S. Young, "HMM based architecture for face identification," *Image, Vision Computing*, vol. 12, pp. 537-583, 1994.
- [9] D. Blackburn, J. Bone, and P. Phillips, "FRVT 2000 evaluation report," Evaluation Report NIST, pp.1-70, February 2001.
- [10] M. Bone and D. Blackburn, "Face recognition at a chokepoint: scenario evaluation results," *Evaluation Report Department of Defense*, November 2002.
- [11] C. Sacchi, F. Granelli, C. Regazzoni, and F. Oberti, "A real-time algorithm for error recovery in remote video-based surveillance application," *Signal Processing: Image Communication*, vol. 17, pp. 165-186, 2002.
- [12] Y. Kim, Joonki Paik, Jingu Heo, Andreas Koschan, Besma Abidi, and Mongi Abidi "Automatic Face Region Tracking for Highly Accurate Face Recognition in Unconstrained Environments," *IEEE Conference on Advanced Video and Signal Based Surveillance*, pp.29-36, 21 July 2003.
- [13] Brown, L.M.; Ying-Li Tian "Comparative study of coarse head pose estimation" *Motion and Video Computing, 2002. Proceedings. Workshop on 5-6 Dec. 2002* Pages:125 - 130
- [14] C. W. Park, Y.O. Kim. H. K. Sung, "Multiple Face Segmentation and Tracking based on Robust Hausdorff Distance Matching" *Int. Journal of Fuzzy Logic and Int. System* June 2003. vol 3. No 1, pp87-92
- [15] Chi, D., Ngan, K.N.: 'Face Segmentation Using Skin-Color map in Videophone Applications, *IEEE Trans. Circuits and systems for video technology*', June,1999, 9, (4), pp. 551-564.
- [16] L. Sirivich and M.kirby, "Low-dimensional procedure for charaterrization of human face," *J. Opt. Soc. Amer.*, vol. 4, pp. 519-524, 1987
- [17] Jun Zhang; Yong Yan; Lades, M, "Pace recognition: eigenface, elastic matching, and neural nets" *Proceedings of the IEEE* , Volume: 85 , Issue: 9 , Sept. 1997 Pages:1423 – 1435
- [18] T. Lee, S. K. Park, M. Kim and M. Park, "Face and Facial Feature Detection under Pose Variation of User Face for human robot interaction, *Information Science, An International Journal*, submitted.